Supporting Information to

Aluminum complexes with redox-active formazanate ligand: Synthesis, characterization, and reduction chemistry

Ranajit Mondol and Edwin Otten*

Stratingh Institute for Chemistry, University of Groningen, Nijenborgh 4, 9747 AG Groningen, The Netherlands

Contents

Experimental Section

Synthesis of [(PhNNC(*p*-tol)NNPh)AlEt$_2$] (2a). 3-*p*-tolyl-1,5-diphenyl-formazan **LH** (20 mg, 0.064 mmol) was dissolved in 0.5 mL of C_6D_6 into a young NMR tube. To this cherry red formazan solution was added triethyl aluminum (10 µL, 0.070 mmol) at room temperature. The color of the solution changed rapidly from cherry-red to dark purple and gas evolution was observed. Then ^{1}H NMR was taken and which indicated the formation of expected product **2a**. ^{1}H NMR (400 MHz, C_6D_6, 25 °C) ^{1}H NMR δ 8.22 (d, *J* = 8.1 Hz, 2H, p-tol *o*-H), 7.71 (d, *J* = 7.8 Hz, 4H, NPh *o*-H), 7.18 (d, *J* = 8.1 Hz, 2H, p-tol *m*-H), 7.08 (t, *J* = 7.8 Hz, 4H, NPh *m*-H), 6.98 (t, *J* = 7.3 Hz, 2H, NPh *p*-H), 2.17 (s, 3H, p-tol CH_3), 1.08 (t, *J* = 8.1 Hz, 6H, AlEt CH_2CH_3), 0.42 (q, *J* = 8.1 Hz, 4H, AlEt CH_2CH_3).

Synthesis of [(PhNNC(*p*-tol)NNPh)Al(Et)I] (3a). Following the same synthetic procedure as mention above compound **2a** was synthesized in a young NMR tube. After that to this NMR tube 2 equiv of Iodine (I_2) was added and let it reacted for 30 hrs at room temperature. ^{1}H NMR indicated the formation of mono-iodo product [(PhNNC(*p*-tol)NNPh)Al(Et)I] **3a** instead of expected diiodide product [(PhNNC(*p*-tol)NNPh)AlI$_2$] **5**. Then NMR tube was heated at 40 °C for 6 hrs and no further conversion was observed. On further heating of NMR tube above 40 °C compound started to decompose. ^{1}H NMR (400 MHz, C_6D_6, 25 °C) δ 8.08 (d, *J* = 8.2 Hz, 2H, p-tol *o*-H), 7.75 (d, *J* = 7.6 Hz, 4H, NPh *o*-H), 7.13 (d, *J* = 8.1 Hz, 2H, p-tol *m*-H), 7.03 (t, *J* = 7.5 Hz, 4H, NPh *m*-H), 6.99 – 6.93 (m, 2H, NPh *p*-H), 2.57 (q, *J* = 7.5 Hz, 2H, EtI), 2.16 (s, 3H, p-tol CH_3), 1.31 (t, *J* = 7.5 Hz, 3H, EtI), 1.02 (t, *J* = 8.0 Hz, 3H, Al(Et)I CH_2CH_3), 0.66 (q, *J* = 8.1 Hz, 2H, Al(Et)I CH_2CH_3).

Synthesis of [(PhNNC(*p*-tol)NNPh)AlMe$_2$] (2b). 3-*p*-tolyl-1,5-diphenyl-formazan **LH** (300 mg, 0.954 mmol) was dissolved in 20 mL of toluene into a Schlenk tube. To this cherry red formazan solution was added trimethyl aluminum (100 µL, 1.049 mmol) at room temperature. The color of the solution changed rapidly from cherry-red to dark purple and gas evolution was observed. The reaction mixture was stirred for overnight at room temperature. After that all the volatiles were removed in vacuo. ^{1}H NMR was taken for the crude products and which indicated the formation of expected product **2b**. The crude products were dissolved in hexane and

kept inside the freeze at -30 °C for crystallization. But, unfortunately no crystalline materials of **2b** were obtained. ^{1}H NMR (400 MHz, C_6D_6, 25 °C) δ 8.21 (d, *J* = 8.2 Hz, 2H, p-tol *o*-H), 7.67 (d, *J* = 8.0 Hz, 4H, NPh *o*-H), 7.18 (d, *J* = 8.2 Hz, p-tol *m*-H), 7.06 (t, *J* = 8.0 Hz, 4H, NPh *m*-H), 6.96 (t, *J* = 7.3 Hz, 2H, NPh *p*-H), 2.17 (s, 3H, p-tol CH_3), -0.25 (s, 6H, Al CH_3).

Synthesis of [(PhNNC(*p*-tol)NNPh)Al(Me)I] (3b). The compound **2b** was dissolved in 0.5 mL of C_6D_6 into a young NMR tube. After that to this NMR tube 2 equiv of Iodine (I_2) was added and let it reacted for 24 hrs at room temperature. ^{1}H NMR indicated the formation of mono-iodo product [(PhNNC(*p*-tol)NNPh)Al(Me)I] **3b** instead of expected diiodide product [(PhNNC(*p*-tol)NNPh)AlI_2] **5** and the present of starting material **2b**. On heating the NMR tube at 80 °C compound started to decompose.^{1}H NMR (400 MHz, C_6D_6, 25 °C) δ 8.21 (d, *J* = 8.2 Hz, 1H, p-tol *o*-H (**2b**)), 8.10 (d, *J* = 8.2 Hz, 2H, p-tol *o*-H (**3b**)), 7.71 (d, *J* = 8.2 Hz, 4H, NPh *o*-H (**3b**)), 7.67 (d, *J* = 8.2 Hz, 2H, NPh *o*-H (**2b**)), 7.18 (d, *J* = 8.2 Hz, 1H, p-tol *m*-H (**2b**)), 7.13 (d, *J* = 8.2 Hz, 2H, p-tol *m*-H (**3b**)), 7.06 (t, *J* = 8.0 Hz, 2H, NPh *m*-H (**2b**)), 7.03 – 6.97 (m, 6H, overlapped, NPh (*m*+*p*)-H (**3b**)), 6.96 (t, *J* = 7.3 Hz, 1H, NPh *p*-H (**2b**)), 2.17 (s, 1.5H, p-tol CH_3 (**2b**)), 2.16 (s, 3H, p-tol CH_3 (**3b**)), 0.30 (s, 3H, MeI), 0.17 (s, 3H, Al CH_3 (**3b**)), -0.25 (s, 3H, Al CH_3 (**2b**)).

Cyclic Voltammetry

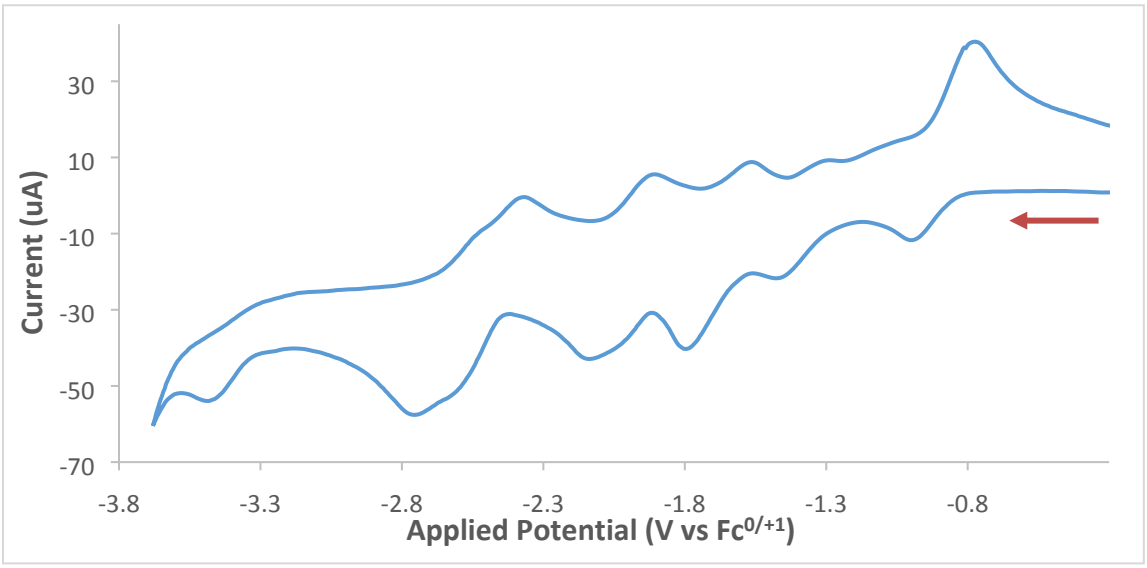

Figure S1. Cyclic voltammetry of **1** (1.5 mM solution in THF, 0.1 M $[Bu_4N][PF_6]$) recorded at 100 mVs^{-1}

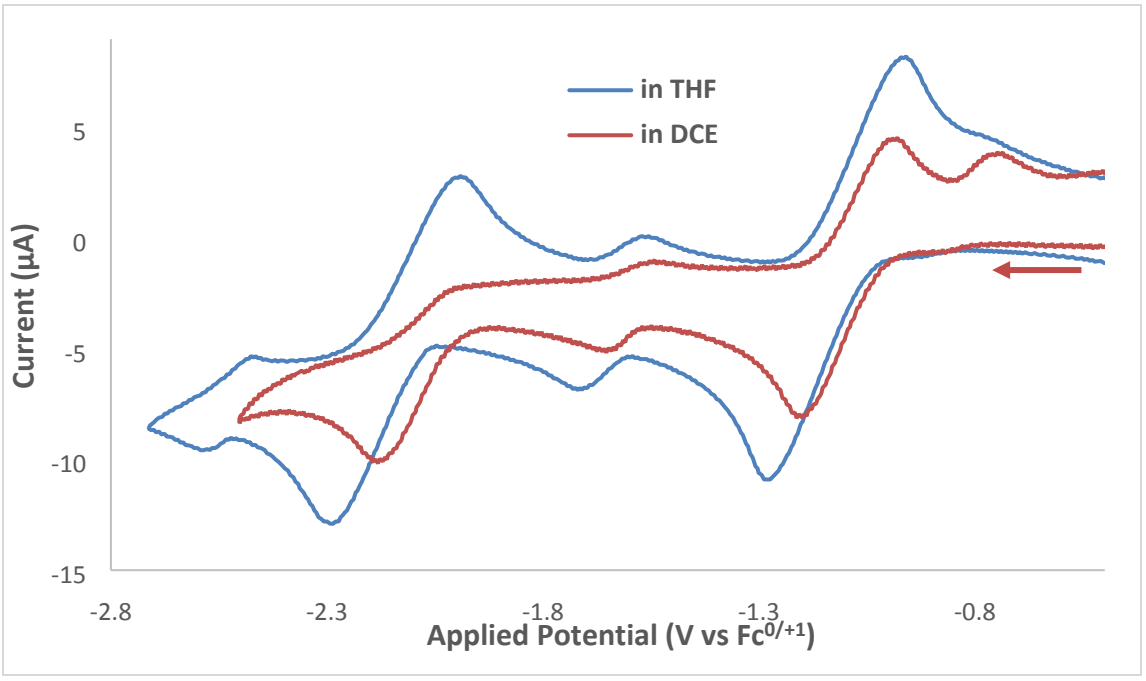

Figure S2. Cyclic voltammetry of **4** in THF (**blue**) and in DCE (**red**) [2.5mM **4,** 0.1M Bu_4NPF_6] recorded at 100 mVs^{-1}

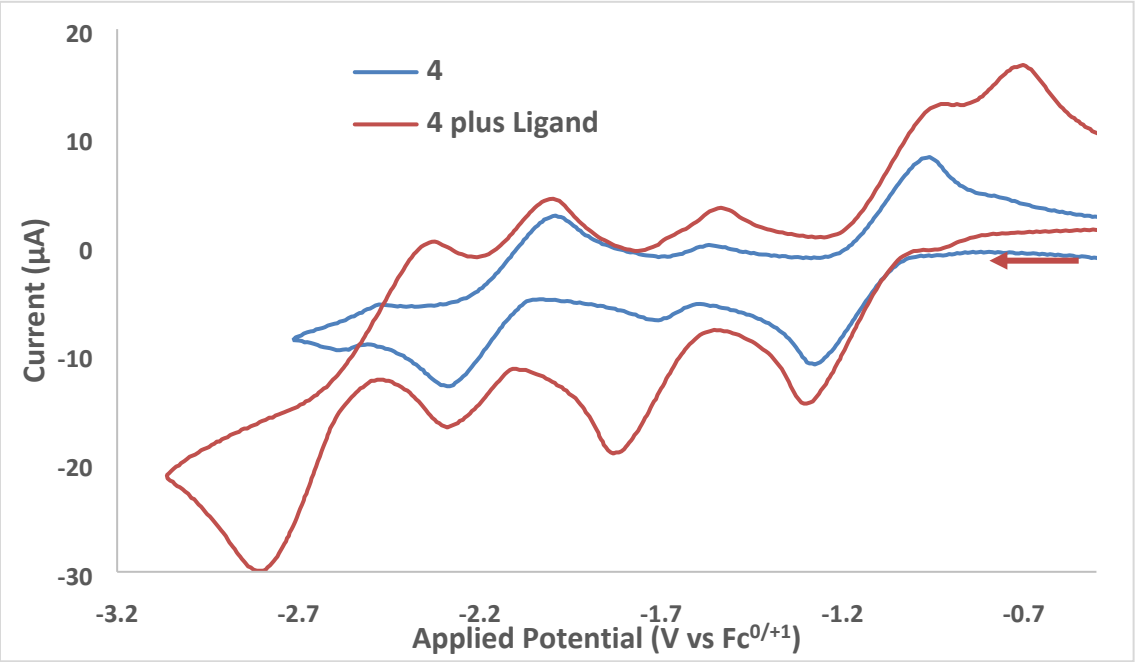

Figure S3. Cyclic voltammetry of **4** in THF [2.5mM **4,** 0.1M Bu_4NPF_6] recorded at 100 mVs^{-1} (**blue**: before addition of free ligand, **red**: after addition of free ligand)

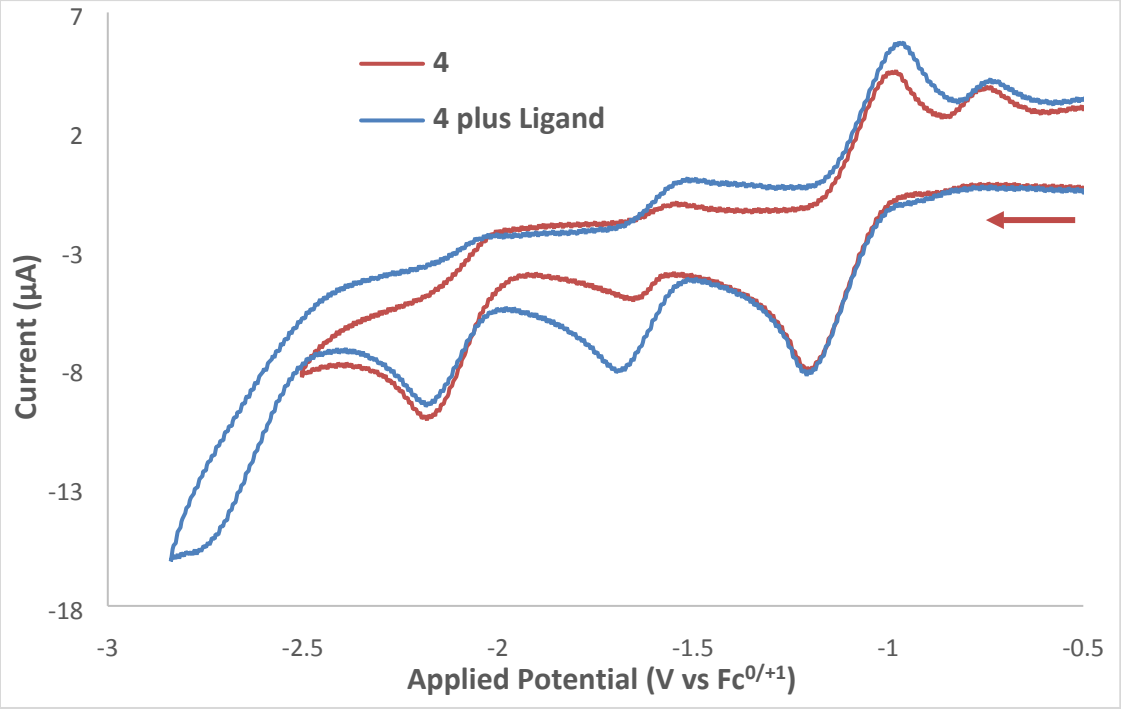

Figure S4. Cyclic voltammetry of **4** in DCE [2.5mM **4,** 0.1M Bu_4NPF_6] recorded at 100 mVs^{-1} (**red**: before addition of free ligand, **blue**: after addition of free ligand)

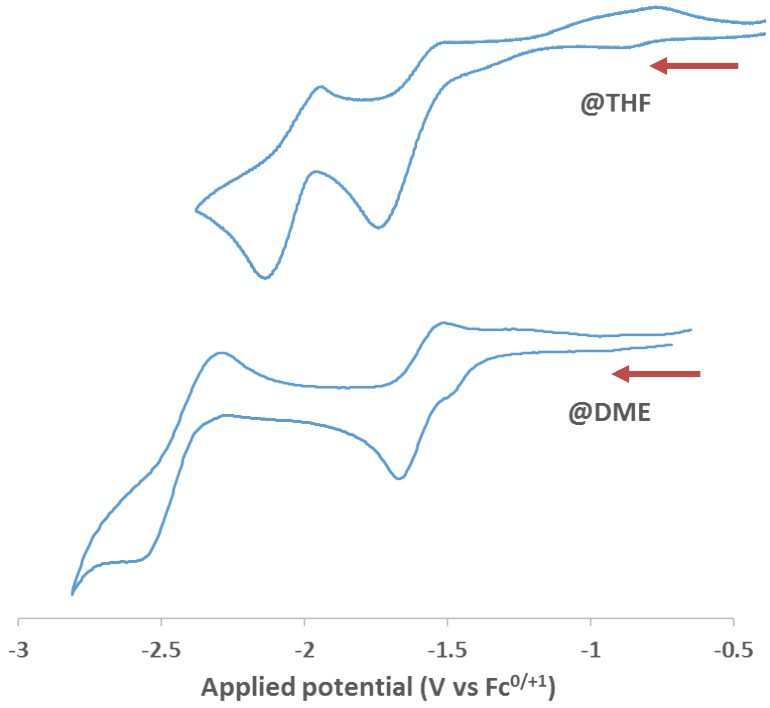

Figure S5. Cyclic voltammetry for **5** [2.5mM **5,** 0.1M Bu_4NPF_6] recorded at 100 mVs^{-1} in THF (top) and in DME (bottom)

In contrast to the data for the diphenyl complex **4**, the voltammogram of the aluminum iodide **5** measured in either THF or DME solution is poorly reversible and shows reduction events that are shifted to more negative potentials (Figure S5 and Table S1). The changes in electrochemistry upon changing the Al-substituents from Ph to I may reflect the lability of the Al-I bond upon reduction. The peak potential difference between the 1st and 2nd reduction peaks ($\Delta E_{pa} = E_{p,a1} - E_{p,a2}$) for **4** in THF is ca. 1.0 V, whereas the corresponding difference for **5** in THF and DME are ca. 0.37 and 0.89 V, respectively. The very small ΔE_{pa} value for **5** in THF may be due to loss of I^- upon reduction to form the neutral radical $[LAl(I)(THF)]^{\cdot}$ as its THF adduct. The difference between THF and DME is likely due to the difference in coordinating ability between these two solvents. We propose that loss of I^- does not occur in DME, and the second reduction forms $[LAlI_2]^{2-}$ directly without the intermediacy of a neutral radical such as in THF (Scheme S1).

Table S1. Electrochemical data for compounds **4** and **5**

Compounds	Solvents	1st reduction potential vs $Fc^{0/+1}$ (V)	2nd reduction potential vs $Fc^{0/+1}$ (V)	$\Delta E_{p,a}$ (V)
4	THF	-1.13	-2.14	1.0
5	THF	-1.75 (peak potential)	-2.12 (peak potential)	0.37
5	DME	-1.67 (peak potential)	-2.56 (peak potential)	0.89

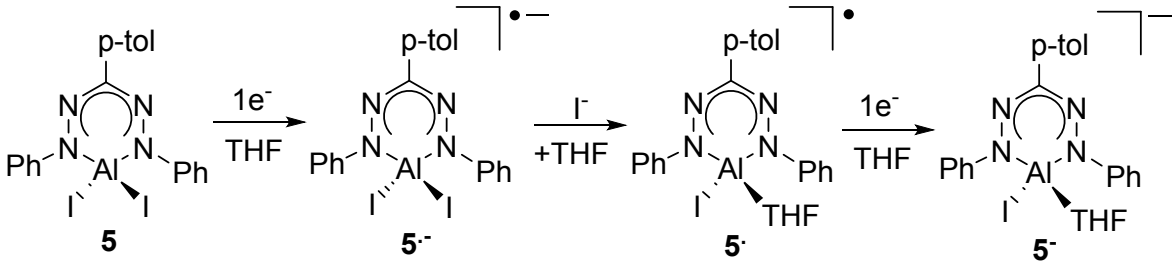

Scheme S1. Schematic depiction of electrochemical processes in THF solution of **5**

EPR Spectroscopy

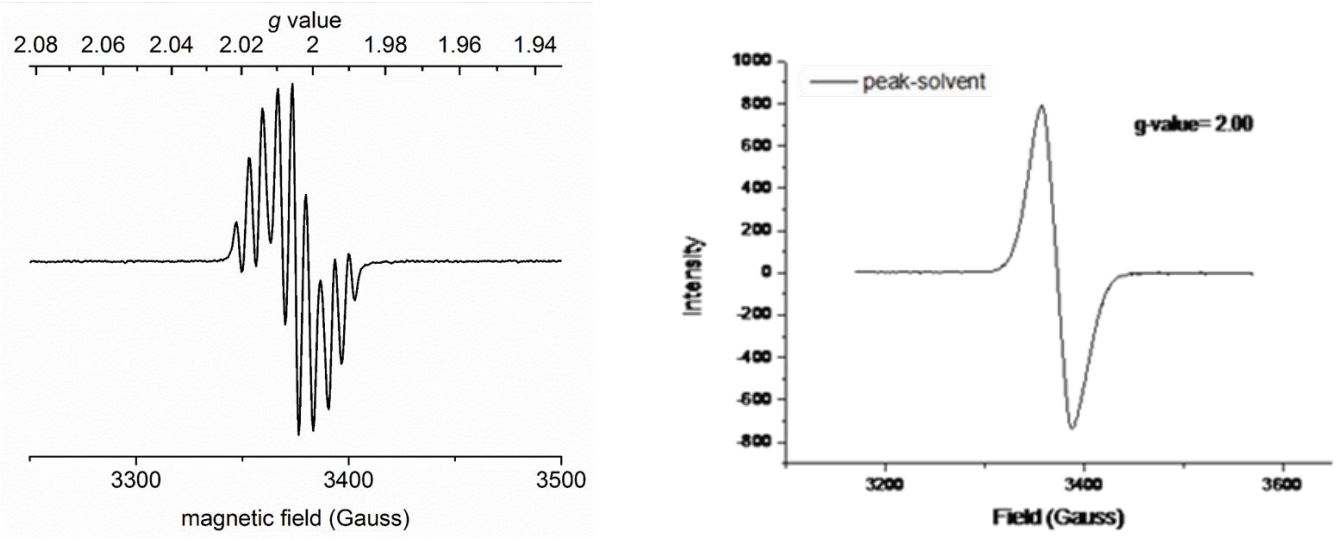

Figure S6. EPR spectrum of $\mathbf{1}^{-\cdot}$ in (THF) (left) and $\mathbf{4}^{-\cdot}$ in DCE at room temperature

UV/Vis Spectroscopy

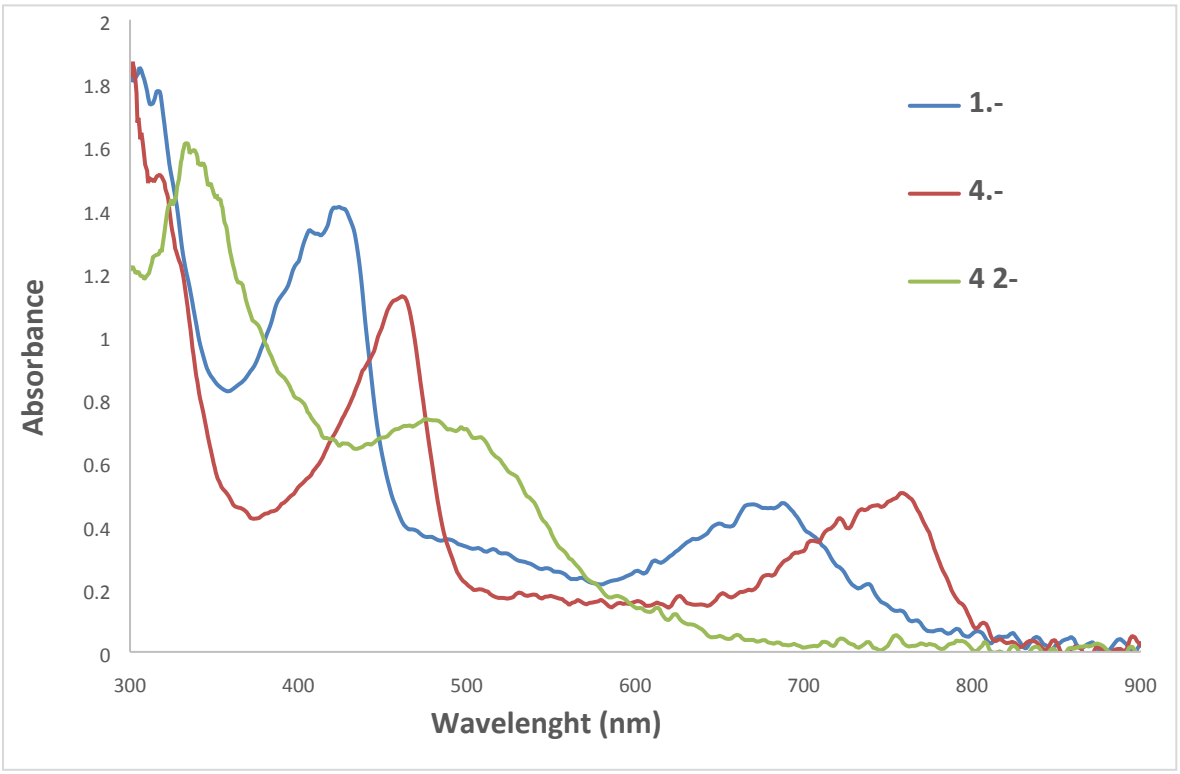

Figure S7. Absorption spectra of compounds $\mathbf{1}^{\cdot-}$ (in THF), $\mathbf{4}^{\cdot-}$ (in DCE) and $\mathbf{4}^{2-}$ (in THF)

NMR Spectra

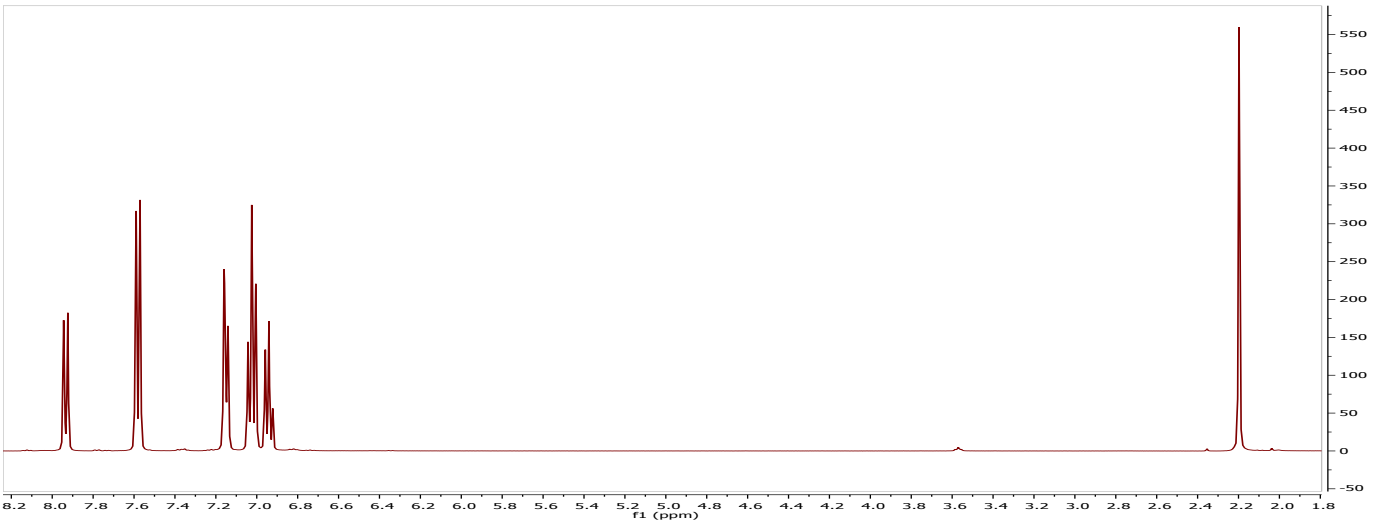

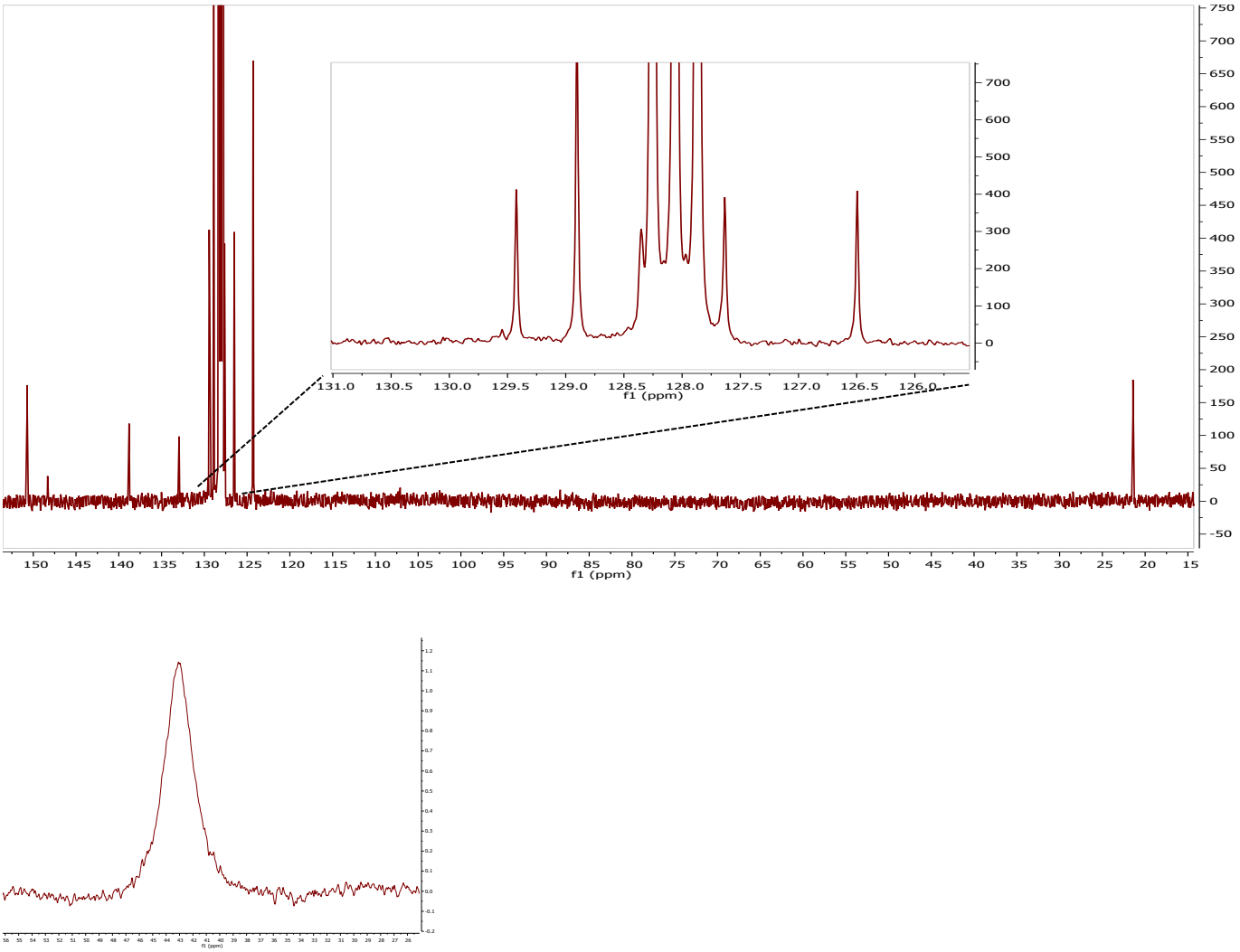

Figure S8. ^{1}H NMR (top), ^{13}C NMR (middle) and ^{27}Al NMR (bottom) at 25 °C of **1** in C_6D_6

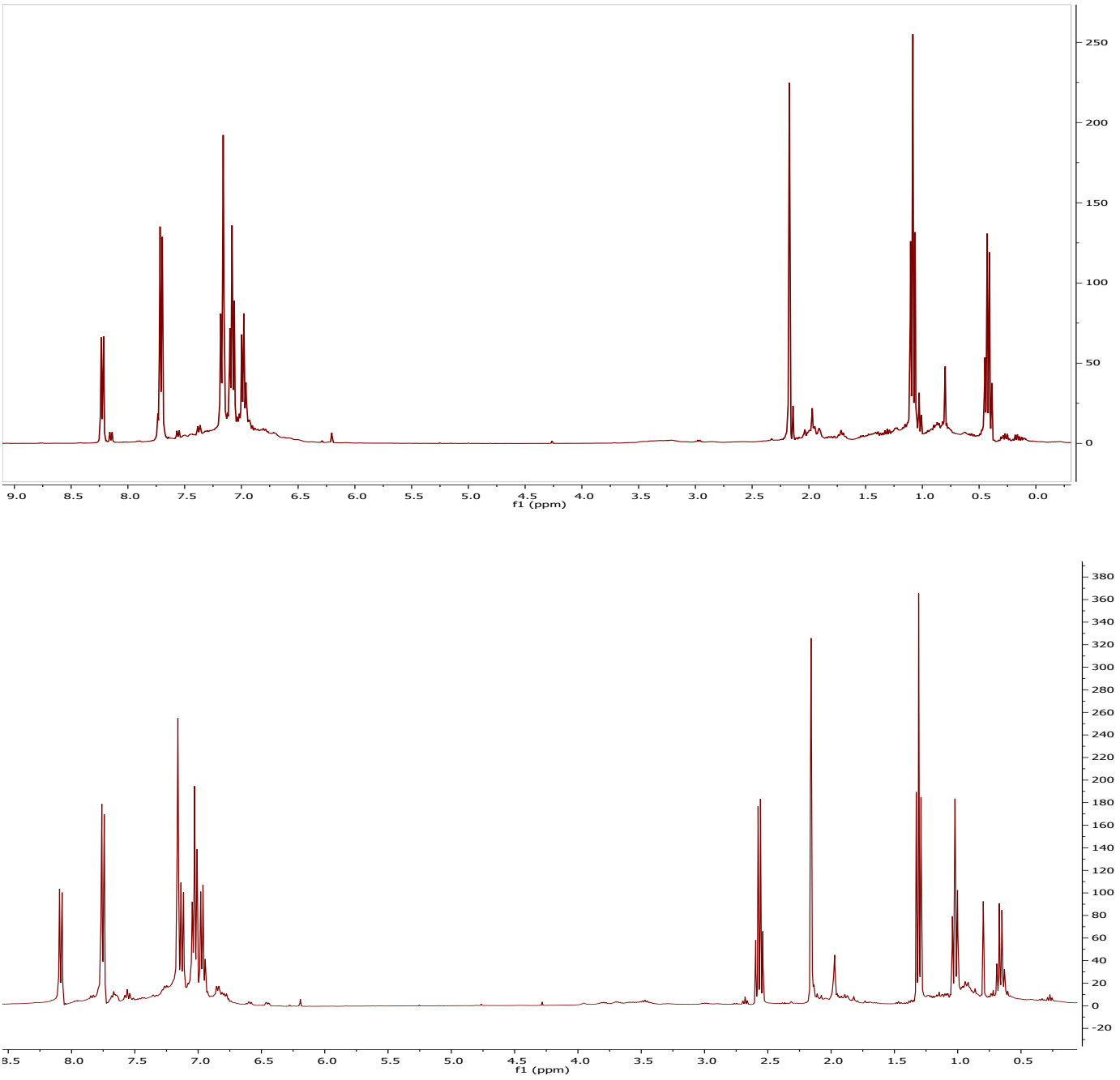

Figure S9. Compounds **2a** and **3a** were generated in young NMR tube. ^{1}H-NMR of **2a** (shown NMR spectra is the crude product of **2a** without further purification) (top) and ^{1}H-NMR of **3a** (the compound **3a** was generated in-situ from the crude product of **2a** and shown NMR spectra is the crude product of **3a** without further purification) (bottom) in C_6D_6 at 25 °C

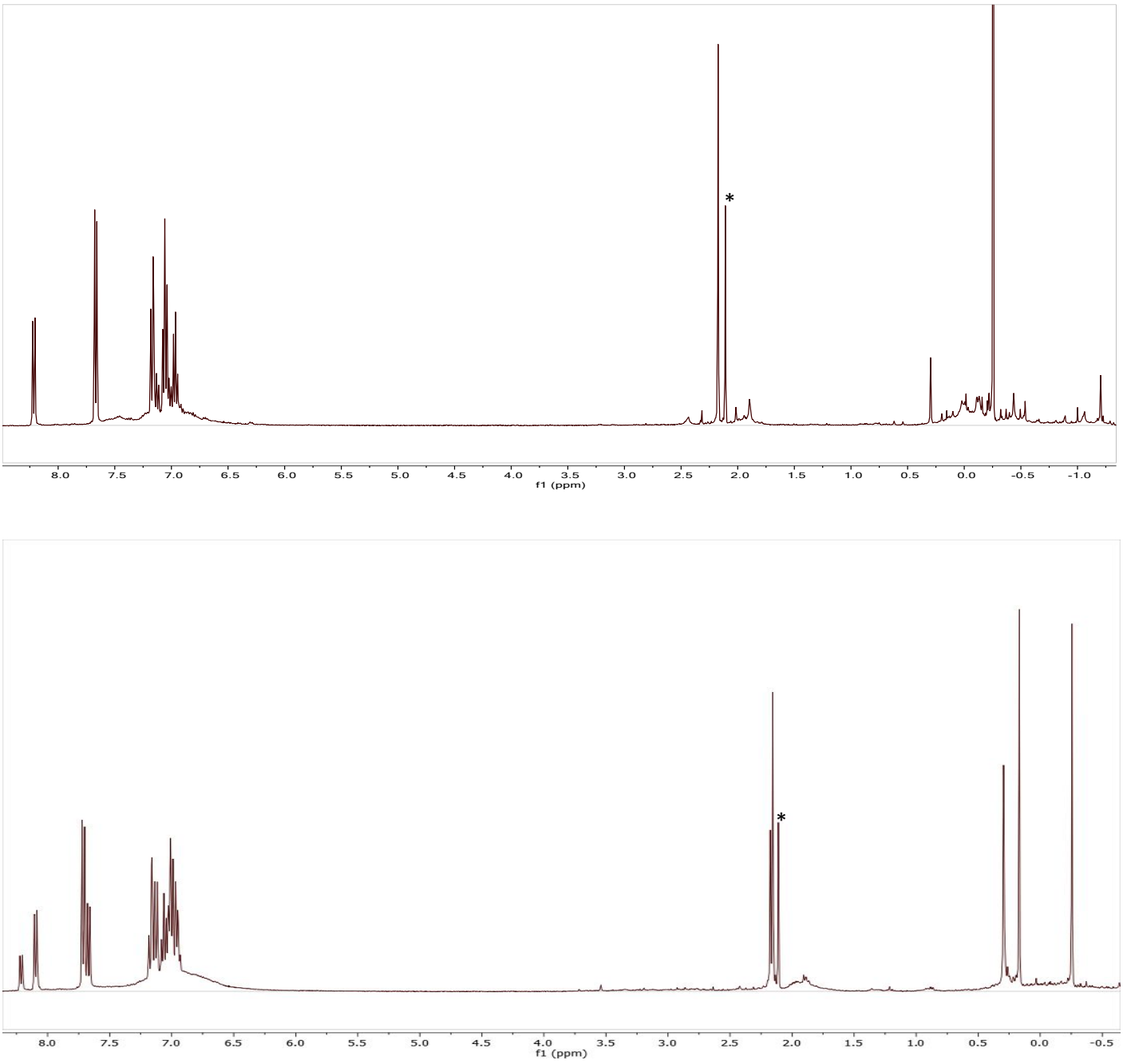

Figure S10. ^{1}H-NMR of **2b** (shown NMR spectra is the crude product of **2b** without further purification) (top, asterisks indicate residual toluene) and ^{1}H-NMR of **3b** (the compound **3b** was generated in young NMR tube by the treatment of the C_6D_6 solution of crude product of **2b** with 2 equivalents of Iodine (I_2) and shown NMR spectra is the crude product of **3b** without further purification) (bottom, asterisks indicate residual toluene) in C_6D_6 at 25 °C

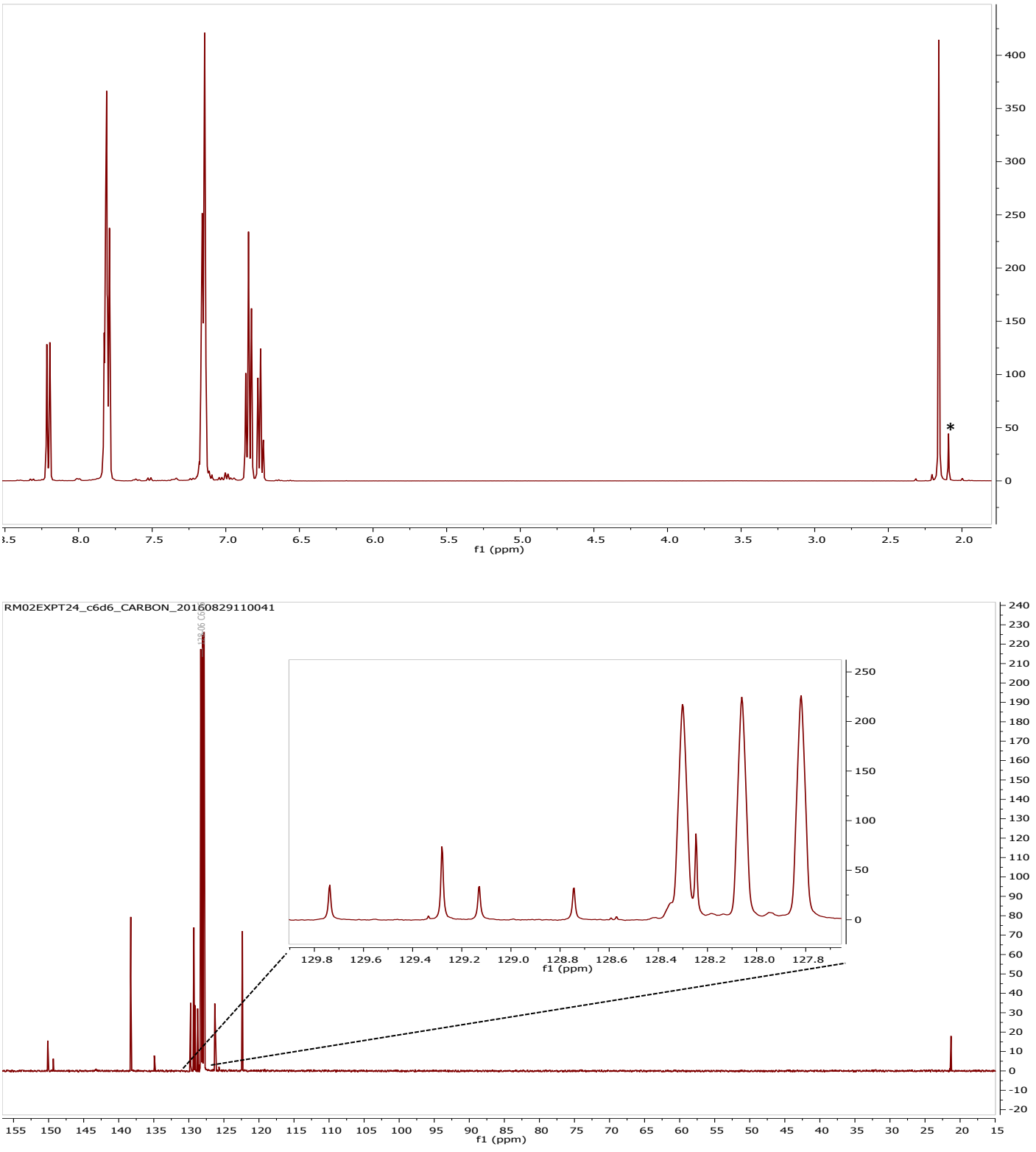

Figure S11. ^{1}H NMR (at 25 °C) (top, asterisks indicate residual toluene) and ^{13}C NMR (at 25 °C) (bottom) of **4** in C_6D_6

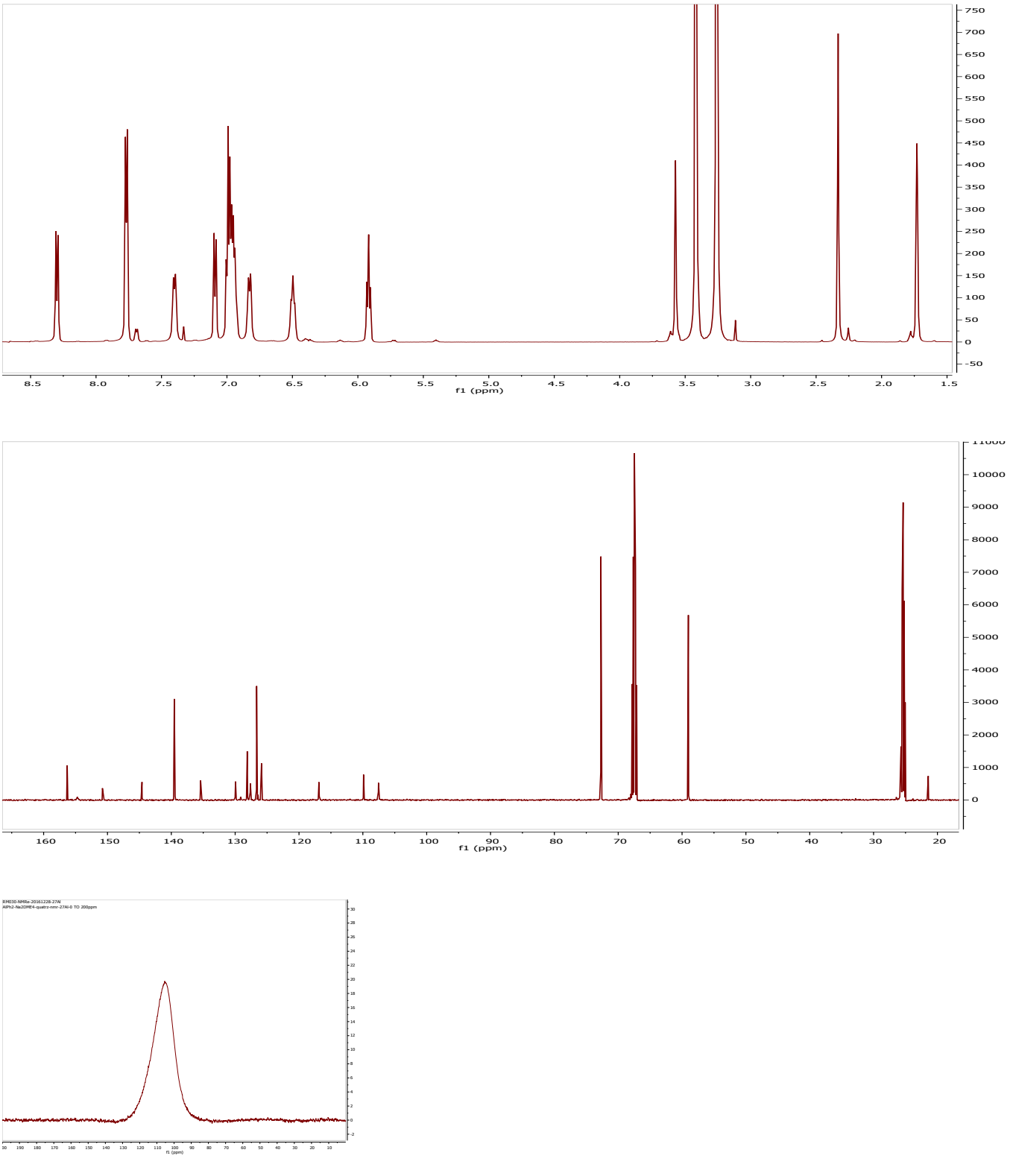

Figure S12. ^{1}H NMR (at -30 °C) (Top), ^{13}C NMR (at -30 °C) (Middle) and ^{27}Al NMR (at 25 °C) (Bottom) of **4**$^{2-}$ in THF-d_8

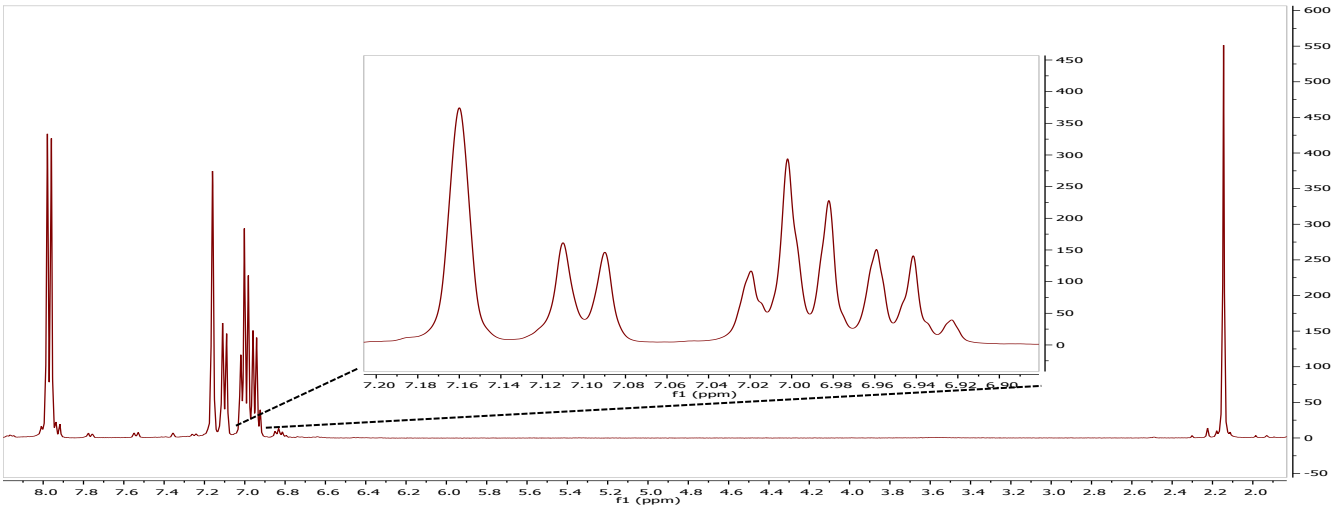

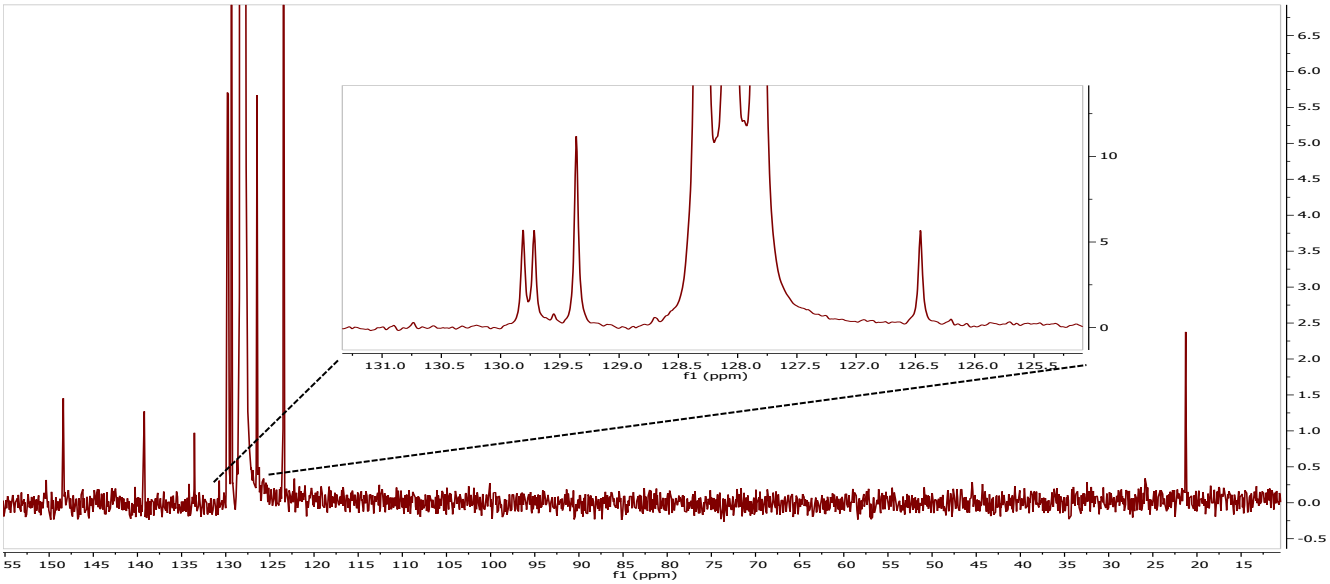

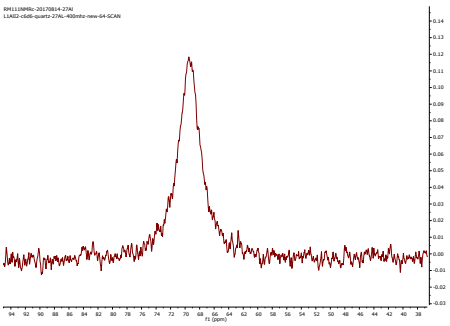

Figure S13. ^{1}H NMR (at 25 °C) (top), ^{13}C NMR (at 25 °C) (middle) and ^{27}Al NMR (at 25 °C) (bottom) of **5** in C_6D_6

Computational Data

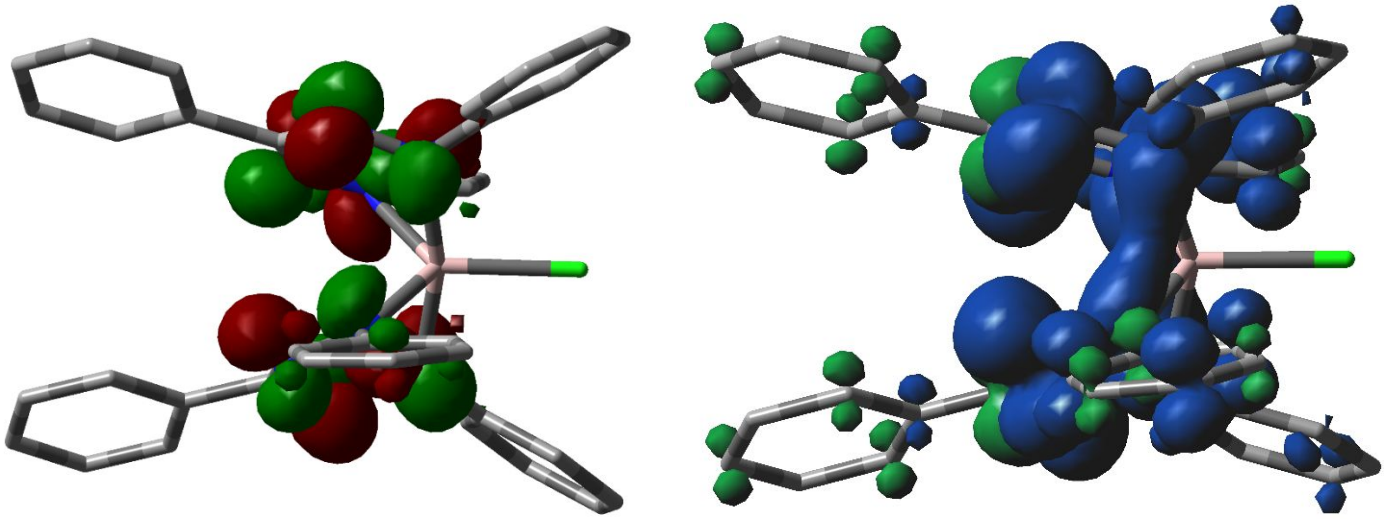

Figure S14. LUMO of $\mathbf{1}_{calc}$ (left) and spin density plot of $\mathbf{1}^{-\cdot}{}_{calc}$ (right)

Table S2. Selected bond lengths values (Å) and bond angles values (°) for **1**, $\mathbf{1}_{calc}$ and $\mathbf{1}^{-\cdot}{}_{calc}$

Bonds	**Bond lenghts**			**Angles**	**Bonds angles**		
	1	$\mathbf{1}_{calc}$	$\mathbf{1}^{-\cdot}{}_{calc}$		**1**	$\mathbf{1}_{calc}$	$\mathbf{1}^{-\cdot}{}_{calc}$
Al1 -Cl1	2.143(1)	2.163	2.196	N1-Al1-N8	165.22(1)	165.872	155.128
Al1 -N1	1.999(4)	2.049	2.038	N1-Al1-Cl1	97.72(1)	97.063	102.436
Al1 -N8	2.007(4)	2.049	2.038	N1-Al1-N4	81.29(1)	81.33	82.123
Al1 -N4	1.923(3)	1.953	1.968	N8-Al1-Cl1	97.03(1)	97.065	102.436
Al1 -N5	1.921(3)	1.953	1.968	N8-Al1-N5	81.89(1)	81.332	82.123
N1-N2	1.316(4)	1.291	1.327	N4-Al1-N5	106.65(1)	109.288	128.33
N7-N8	1.307(4)	1.291	1.327	Cl1-Al1-N4	127.10(1)	125.352	115.84
N3-N4	1.320(4)	1.31	1.338	Cl1-Al1-N5	126.25(1)	125.36	115.84
N5-N6	1.322(4)	1.31	1.338	Al1-N1-N2	118.48(3)	118.732	116.267

N2-C7	1.350(5)	1.349	1.343	Al1-N1-C1	130.36(3)	129.317	129.63
N7-C27	1.352(5)	1.349	1.343	N2-N1-C1	110.65(3)	111.139	111.068
N6-C27	1.342(5)	1.336	1.342	Al1-N8-N7	118.31(3)	118.736	116.268
N3-C7	1.343(5)	1.336	1.342	Al1-N8-C35	129.74(3)	129.311	129.629
N1-C1	1.440(5)	1.442	1.425	N7-N8-C35	110.53(3)	113.14	111.067
N8-C35	1.439(5)	1.442	1.425	Al1-N4-N3	119.64(3)	119.963	116.424
N4-C15	1.436(5)	1.429	1.415	Al1-N4-C15	125.51(3)	125.178	128.061
N5-C21	1.432(5)	1.429	1.415	N3-N4-C15	112.69(3)	113.841	112.664
				Al1-N5-N6	119.48(3)	119.962	116.425
				Al1-N5-C21	124.28(3)	125.179	128.06
				N6-N5-C21	113.75(3)	113.841	112.663

Table S3. Selected bond lengths values (Å) for **4**, $\mathbf{4^{2-}}$ and **5** measured by X-ray crystallography

Bonds	**Bond lengths**		
	4	$\mathbf{4^{2-}}$	**5**
Al1-N1	1.9336(9)	1.871(2)	1.893(2)
Al1-N4	1.9334(8)	1.873(2)	1.900(2)
Al1-C21	1.962(1)	2.011(2)	
Al1-C27	1.957(1)	2.008(2)	
Al1-I1			2.497(7)
Al1-I2			2.494(7)
N1-N2	1.315(1)	1.432(2)	1.317(2)
N3-N4	1.307(1)	1.432(2)	1.313(2)

N2-C7	1.346(1)	1.332(2)	1.344(3)
C7-N3	1.347(1)	1.328(2)	1.346(3)
N1-C1	1.433(1)	1.375(2)	1.432(3)
N4-C15	1.430(1)	1.371(3)	1.433(3)

Table S4. Selected bond angles values (°) for **4**, $\mathbf{4^{2-}}$ and **5** measured by X-ray crystallography

Angles	**Bond angles**		**Angles**	**Bond angles**
	4	$\mathbf{4^{2-}}$		**5**
N1-Al1-N4	90.01(4)	98.54(7)	N1-Al1-N4	92.83(8)
C21-Al1-C27	120.06(5)	107.34(8)	I1-Al1-I2	112.66(2)
C21-Al1-N1	112.96(4)	115.58(7)	I1-Al1-N1	112.65(6)
C21-Al1-N4	112.11(4)	108.46(7	I1-Al1-N4	113.41(6)
C27-Al1-N1	109.57(4)	109.96(7)	I2-Al1-N1	111.34(6)
C27-Al1-N4	108.01(4)	117.14(7)	I2-Al1-N4	112.46(6)
Al1-N1-N2	123.89(7)	122.6(1)	Al1-N1-N2	124.7(1)
Al1-N1-C1	123.57(7)	126.2(1)	Al1-N1-C1	122.6(1)
C1-N1-N2	112.26(8)	111.2(1)	C1-N1-N2	112.7(2)
N3-N4-Al1	124.93(7)	123.6(1)	N3-N4-Al1	123.8(1)
Al1-N4-C15	122.66(7)	125.1(1)	Al1-N4-C15	123.5(1)
N3-N4-C15	112.28(8)	110.9(1)	N3-N4-C15	112.6(2)
N1-N2-C7	121.62(9)	118.6(1)	N1-N2-C7	121.2(2)
N4-N3-C7	121.09(9)	118.1(1)	N4-N3-C7	121.7(2)
N2-C7-N3	129.06(9)	137.2(2)	N2-C7-N3	129.2(2)